Preparation and Characterization of Activated Carbon from Castor Seed Hull with H3po4

Article *in* SSRN Electronic Journal · January 2022

DOI: 10.2139/ssrn.4138328

2 authors:

Ibsa Neme
Addis Ababa Science and Technology University
22 PUBLICATIONS **66** CITATIONS
SEE PROFILE

Girma Gonfa
Addis Ababa Science and Technology University
80 PUBLICATIONS **1,593** CITATIONS
SEE PROFILE

Results in Materials 15 (2022) 100304

Contents lists available at ScienceDirect

Results in Materials

journal homepage: www.sciencedirect.com/journal/results-in-materials

Preparation and characterization of activated carbon from castor seed hull by chemical activation with H_3PO_4

Ibsa Neme [a], Girma Gonfa [a,c,d,*], Chandran Masi [b,c]

[a] Chemical Engineering Department, Addis Ababa Science, and Technology University, 16417 A, Ethiopia
[b] Department of Biotechnology, College of Biological and Chemical Engineering Addis Ababa, Ethiopia
[c] Biotechnology and Bioprocess Center of Excellence, Addis Ababa Science and Technology University, 16417, Addis Ababa, Ethiopia
[d] Nanotechnology Center of Excellence, Addis Ababa Science and Technology University, 16417, Addis Ababa, Ethiopia

ARTICLE INFO

Keywords:
Castor seed hull
Activated carbon
Phosphoric acid
Chemical activation
Thermal activation
Characterization

ABSTRACT

Activated carbon (AC) is an import porous material that is used for various industrial applications. In this work, AC was prepared from the castor seed hull (CH-AC) through H_3PO_4 impregnations and thermal treatments. The raw castor seed hull was treated with H_3PO_4 with various impregnation rations (0.2–0.8), and then thermally treated at 600, 700, and 900 °C for calcination times of 60, 90, and 120 min. The resulting activated carbons were characterized using SEM, XRD, FTIR, TGA, and BET. The activated carbon yield of the CH-AC at various activation conditions was determined. The proximate and ultimate analyses, morphological and textural properties of the AC were measured. The effects of H_3PO_4 impregnation ratio, activation time, and activation temperature on the AC yield, and morphological and textural properties were investigated. The yield of the AC increases with increasing H_3PO_4 impregnation ratio and a maximum AC yield of 78.86%, was obtained at $0.8H_3PO_4$ impregnation ratio, activation temperature of 700 °C, and activation time of 60 min. Moreover, a maximum BET surface area of 785.38 m^2/g was obtained at $0.8H_3PO_4$ impregnation ration 78.86%, activation temperature of 700 °C, and activation time of 60 min. In this work, we managed to prepare AC with good yield and textural characteristics using low H_3PO_4 implementation ratio which could lower the cost of production of activated carbons from biomass.

1. Introduction

Activated carbon (AC) is the most commonly used porous carbonaceous material because of its highly developed surface area and availability. Its high surface area, well-organized micro, and mesopores with a wide range of functional groups make AC a versatile material with numerous applications [1]. AC has a very broad range of applications in different industries, such as gas separation and storage [2–4], water treatments [5,6], industrial purifications [7], medical application [8], catalyst and catalyst support [9], and super-capacitors and electrodes [10–12]. AC is prepared from carbon-rich precursors, such as coal [13] or biomass [1,14,15]. At the early stage of its development AC, coal was widely used as a precursor for the preparation of AC. Due to limited coal reserves, other carbon-rich precursors, such as biomass or other carbon-rich precursors were used. Preparations of AC from biomass have many advantages. The precursors are diverse, low-cost, abundant, and renewable [14,16]. Moreover, due to its reactivity, the preparation of AC from biomass precursors is relatively [14]. AC from biomass precursors also shows excellent surface properties with a high degree of porosity and a high specific surface area [16]. Further, the utilization of waste biomass for the production of AC contributes to decreasing costs of waste disposal and the negative impact on the environment [14,15].

Several biomasses and biomass wastes have been investigated for the synthesis of AC. These include wood and woody materials such as eucalyptus, jatropha, acacia mangium woods [17] or fruit shells, fruit stones, and fruit hull [18–20]. Some of the fruit hulls used for the synthesis of AC are jatropha hulls [19], oat hulls [21], peanut hulls [22], rice hulls [15], and corn hulls [23]. Previous studies show that the properties, quality, and quantity of the AC obtained from various biomass procurers depend on the nature of the biomass, preparation methods, and activation conditions [1,14,15,24]. For good development of AC with high surface area, good structural and textural characteristics, biomass with high fixed carbon content,t and low ash continent are desirable [14,15].

* Corresponding author. Chemical Engineering Department, Addis Ababa Science, and Technology University, 16417 A, Ethiopia.
E-mail address: kiyyaagonfaa@gmail.com (G. Gonfa).

https://doi.org/10.1016/j.rinma.2022.100304
Received 31 May 2022; Received in revised form 24 June 2022; Accepted 13 July 2022
Available online 21 July 2022

In this work, AC was synthesized from castor bean seed hull using phosphoric acid (H_3PO_4) treatment followed by thermal activation. Castor bean plant (Ricinus communis) belongs to the Euphorbia family (Euphorbiaceae) which is native to Ethiopia and has become naturalized in tropical and warm temperate regions of the world [25,26]. The world's caster seeds production and consumption have been increasing in recent years. The world consumption of castor oil increased by about 50% in 25 years; from around 400,000 tons in 1985 to 610,000 tons in 2010 [27]. In 2017, the world production of castor seeds reached 1,791, 409 tons [28]. Castor oil production generates large number of by-products/residues during processing. Hence, investigation of castor bean oil residue, such as its husk has paramount importance both for economic and environmental aspects.

Previously, the syntheses of AC from castor seed cake were investigated [28–31]. Aldobouni et al. [29] synthesized AC from char resulting from the pyrolysis of de-oiled castor seed cake by treating with H_3PO_4) and $ZnCl_2$ followed by thermal treatment. Zhi and Zaini [32] prepared AC from castor bean residue by impregnating it with metal chloride and thermal treatment. Ospina et al. [30] used K_2CO_3 and thermal treatment for the synthesis of AC from de-oiled castor cake. Sánchez-Cantú et al. [31] used castor cake for the preparation of AC using K_2CO_3 and thermal treatments. Recently, Ferreira et al. [28] synthesized AC from castor seed cake by impregnating it with H_3PO_4 followed by thermal treatment. These studies show that AC prepared from caster been residues has good characteristics and can be used for various applications, such as catalyst support [30] and removal of pollutants from water, such as methylene blue [28,31], rhodamine B [32].

In our current work, we used castor seed hull for the synthesis of AC through H_3PO_4 treatment followed by thermal treatment. To the best of our knowledge, there are no previous reports on preparation of activated carbon from castor seed hulls. Phosphoric acid has been wide as chemical activation due to its less environmental and economic concerns [17,28]. Phosphoric acid chemically links to the biomass polymers and introduces phosphate groups forming crosslinks [28]. Moreover, H_3PO_4 prevents the loss of biomass through volatilization during thermal action, thus increasing the AC yield from carbonization [28]. In this work, AC was produced from a castor seed hull using chemically phosphoric acid as an activating agent. The effects of acid concentration, carbonization temperature, and carbonation time on AC yield, surface area, pore size distribution, pore diameter, pore-volume, and surface morphology were studied.

2. Materials and methods

2.1. Materials and chemicals

Castor capsule beans were collected from the Akaki Kaliti area, Addis Ababa, Ethiopia, and was used as precursor. Reagent grade phosphoric acid and sodium hydroxide were used. Castor seed hulls were removed from the castor capsule bean using a knife and washed with water to remove dirties. The weight of the seed bean and castor seed hull was measured using analytical mass balance. The weight of the seed hull on the castor capsule bean was 42.1%. The washed seed hull was then oven-dried at 100 °C for 24 h. The dried sample was crushed using a high-speed multi-functional crusher (M-1000A) and sieved to the required particle size. The sample was stored in plastic bags for further experiments.

2.2. Preparation of activated carbon

The chemical activation of CS was performed with H_3PO_4 as an activating agent. The initial density and concentration of H_3PO_4 used 1.71 g/mL and 85% (w/v), respectively. The castor seed hull activated carbon preparation was carried out using previously reported procedures with some modifications [17,18,33]. Castor seed hull powder (50 g) was mixed with 200 mL distilled water at 25 °C for 4 h under stirring. Assuming that all the acid was incorporated with the raw precursor, the impregnation ratios (X_p) were calculated using equation (1) as the ratio of H_3PO_4 weight in solution to the weight of the dried Castor seed hull powder [17]. Hence, the X_p values are 0.25, 0.5, and 0.8. The excess water was evaporated in the oven (100 °C) to ensure complete absorbance of the acid onto the castor seed hull powder. Then, H_3PO_4-impregnated samples were activated in a muffle furnace (FE-37-FA-013) at 600 °C, 700 °C, and 800 °C for carbonation times (60, 90, and 120 min). The calcination temperatures were selected based on a preliminary thermal property assessment of the raw cater bean husk using TGA analysis. Calculations were performed under a nitrogen flow rate of 150 mL/min and at a heating rate of 10 °C/min. Finally, the activated carbons were cool to room temperature, washed with 1 M NaOH, and successively rinsed with distilled water to remove the remaining chemicals until the pH of the washing effluent was reaches 6.0 to 7.0. The resulting activated carbons were dried in an oven at 100 °C for 12 h and stored in plastic containers.

$$X_p = \frac{H_3PO_4\ weight}{Dired\ precurser\ weigh} \quad (1)$$

2.3. Characterization

The proximate analyses of dried castor seed hull (CS) powder and the synthesized activated carbon (CS-AC) were carried out according to ASTM E 870-82), and the ultimate analyses were performed using ASTM D3176-89. Similarly, the ash contents of CS and CSAC were determined according to ASTM D2866-94 standard method. The ultimate analyses (C, H, N, and O elements) were determined using EA 1112 Flash NS/O-elemental analyzer. Thermogravimetric analyses were carried out using SDT Q600 thermogravimetric analysis (TGA). The surface functional groups of raw castor seed hull and acid-treated AC were analyzed using Fourier transform infra-red (FTIR) spectroscopy (FTIR-is50ABx). A scanning electron microscopy (SEM inspect F50 USA) device was used to observe the surface morphology of activated carbon. The x-ray diffraction of the precursor (RCH) and the resulting activated carbon (CH-AC) were measured with an x-ray diffractometer (XRD-7000). The BET surface area, micropore volume, and micropore surface area of the activated carbons were determined by application of the Brunauer-Emmett-Teller (BET).

3. Results and discussion

3.1. Proximate and ultimate analyses

Proximate analysis of the raw castor seed hull (CH) and its corresponding activated carbon (CH-AC) treated with H_3PO_4 with an impregnation ratio of 0.8 and carbonation time of 90 min are shown in Table 1. The moisture content of the CS is 4.4% which is comparable with other biomass-based activated carbon precursors, such as durian shell (5.53%) [34] and tomato stems (3.58%) [35], fox nuts (4.00%) [36], etc. (Table 3). Many raw biomasses contain higher moisture depending on the nature of the biomass and pretreatment methods used [14]. The moisture contents of the prepared activated carbons are 6.32, 7.32, and 8.53% for AC activated at 600, 700, and 700 °C. The value obtained for the current AC was slightly higher than AC prepared from other biomass precursors (Table 4). The increased moisture content of

Table 1
Proximate analyses (% wt.) of raw castor seed hull and its activated carbons impregnated with $0.8H_3PO_4$ impregnation ratio and 90 min carbonation time.

	Moisture	Volatile	Ash	Fixed carbon
RCH (precursor)	4.4	72.05	6.71	16.84
CH-AC-600 °C	8.53	54.95	10.97	25.6
CH-AC-700 °C	7.32	52.91	18.07	21.7
CH-AC-800 °C	6.32	49.56	19.10	25.02

Table 2
Ultimate analysis of raw castor seed hull and its activated carbons impregnated with 0.8H3PO4 impregnation ratio and 90 min carbonation time.

	C	H	N	O
Precursor	44.23	5.49	0.22	50.10
AC-600 °C	61.58	3.15	0.50	34.77
AC-700 °C	63.32	2.76	0.74	33.20
AC-800 °C	63.88	3.13	0.52	32.47

the activated carbon may be attributed to its affinity for water molecules compared to its procurer.

The values of volatile matters decrease from 72.05% (for raw castor hull) to 49.56% for AC-800 °C impregnated with H_3PO_4 with an impregnation ratio of 0.8 and 90-min carbonation time. The volatile component composition of the current precursor is comparable with the values reported for other biomass precursors (Table 3). On activation, the composition of the volatile component was reduced while the compositions of fixed carbon and ash content are increased as expected. The composition of the volatile components of the current precursor is comparable with the values reported for other biomass precursors, however, the volatile component in the resulting activated carbon is higher than the value reported for other biomass-based activated carbons (Tables 3 and 4). This might be due to the use of low impregnation ratio used in the current works. In many previous reports higher H_3PO_4 imagination ratio, usually more than 1, was used [17,36]. The ash content of the raw castor hull was slightly higher than the values for the biomass depicted, and lower than the values reported for some biomasses such as tomato stems (10.6%) and tomato leaves (25.72%) [35]. The ash content of the current AC is comparable with the values reported for durian shells (22.36%) [34], higher than the values reported for biomasses [14]. Moreover, it can be observed that higher temperature ash and fixed carbon contents are higher for the current activated carbon. The fixed carbon of the current precursor is also compared with the values reported for most biomasses. However, the compositions of the fixed carbon in CH-AC are much lower than the values reported for activated carbons prepared from other biomasses.

The ultimate analyses of the RCH and resulting CH-AC are depicted in Table 2. As it can be seen, the carbon content of RCH was 44.23% and the values for the activated carbons are 61.58%, 63.32%, and 63.87% for AC-600 °C, AC-700 °C, and AC-800 °C. respectively. On the other hand, the oxygen content decreased from 50.06% for RCH to 32.5% for AC-800 °C. The carbon content of the RCH is 44.23% which is comparable with that of most precursors shown in Table 3. Higher carbon in biomass is characteristic of a good precursor for obtaining good quality and optimum yield of AC [37]. The carbon content of the activated carbon is also comparable with other activated carbons obtained from other biomasses (Table 4).

3.2. SEM and FTIR analyses

Scanning electron microscopy (SEM) was used to observe the surface physical morphology of the RCH and the resulting activated carbon samples. The SEM images of RCH and CH-AC samples prepared with $0.8H_3PO_4$ impregnations and calcination time ratio are shown in Fig. 1. The surface of RCH seed hull shows frizzy image, with less pores and hollow structures (Fig. 1(a)). In the case of ACH samples, more openings and hollow structures were observed (Fig. 3(b–d). As activation temperature increases more irregular pores shapes were obtained on the CH-AC.

The chemical functional groups on the raw castor bean hull and its activated carbon surface were identified with FTIR (Fig. 2). The FTIR spectra were recorded over 4000 to 400 cm^{-1} wavenumber ranges. As can be seen from Fig. 2 (a), the raw castor seed hull shows a wide spectrum over 3500-3250 cm^{-1} due to –OH and N–H groups [18]. The peak at 2904 cm^{-1} represents C–H stretching in the alkane group and the one located at 1733 cm^{-1} corresponds to C═O stretching [39]. Moreover, the peaks located between 1600 and 1500 cm^{-1} (vibration of C═C in aromatic rings) and 1000-1250 cm^{-1} are due to stretching of C–O or C–O–C in acids, phenols, ethers, esters groups, and 1022 cm^{-1} for P–O–P stretching bonds [40,41]. As can be seen from Fig. 2 (b) the peak at 1579.2 cm^{-1} corresponds to the C═C stretching bond of the aromatic ring, 1376.5 cm^{-1} for stretching of C–O or C–O–C in acids, phenols, ethers, esters groups and 1069.2 cm^{-1} for stretching vibration of P–O–P [42,43]. On acid impregnation and thermal treatment, most of these FTIR peaks are diminished due to the loss of the functional groups with volatile components.

Table 3
Compression of proximate and ultimate analysis of cater oil seed hull with different biomass.

Biomass	Moisture	Proximate analysis (wt.%)			Ultimate analysis (wt.%)					
		Ash	V. M[a]	F.C[b]	C	H	O	N	S	References.
Paulownia wood	3.50	1.05	76.54	18.91	45.83	6.29	47.48	0.40	–	[17]
Acai seed	–	1.75	68.70	24.41	43.29	5.98	47.59	1.29	0.10	[37]
Fox nut	4.00	5.00	70.10	20.90	42.30	4.30	52.51	0.82	0.07	[36]
Durian shell	5.53	2.52	69.59	22.30	60.31	8.47	28.06	3.06	0.10	[34]
Euphorbia rigida	3.00	6.40	76.80	13.80	49.56	5.16	44.08	1.20	–	[38]
Eucalyptus wood	5.00	4.80	80.48	14.65	48.20	6.20	44.10	<0.5	<0.10	[3]
Castor seed hull	4.40	6.71	72.05	16.89	44.23	5.49	50.06	0.22		This work

[C]by difference.
[a] VM: volatile matters.
[b] FC: Fixed carbon.

Table 4
Compression of proximate and ultimate analysis of cater oil seed hull activated carbon with activated carbon obtained from other biomass precursors.

Biomass	Treatments			Proximate analysis (wt.%)			Ultimate analysis (wt.%)					
	Chemical	Thermal	Moisture	Ash	V.M[a]	F.C[b]	C	H	O	N	S	References.
Paulownia wood	H_3PO_4	400 °C	2.30	2.63	17.80	77.27	70.83	3.41	25.76	–	–	[17]
Acai seed	KOH	600 °C	–	4.84	4.84	88.55	84.57	2.49	7.81	1.00		[37]
Fox nut	H_3PO_4	700 °C	3.12	2.12	21.05	73.71	64.85	4.52	29.24	1.24	0.15	[36]
CH-AC	H_3PO_4	800 °C	6.32	19.10	49.56	27.76	63.88	3.13	32.47	0.52		This work

[a] VM: volatile matters.
[b] FC: Fixed carbon.

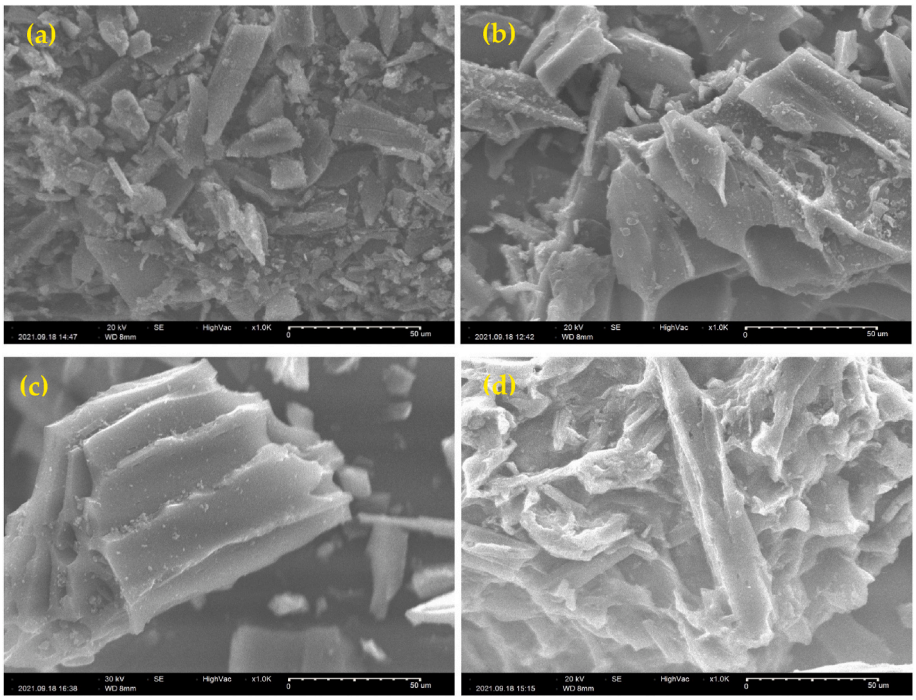

Fig. 1. SEM images. **(a)** RCH and CH-AC activated at 700 °C with H3PO4 impregnation ratio (**b**) 0.25; **(c)** 0.5; and **(d)** 0.8.

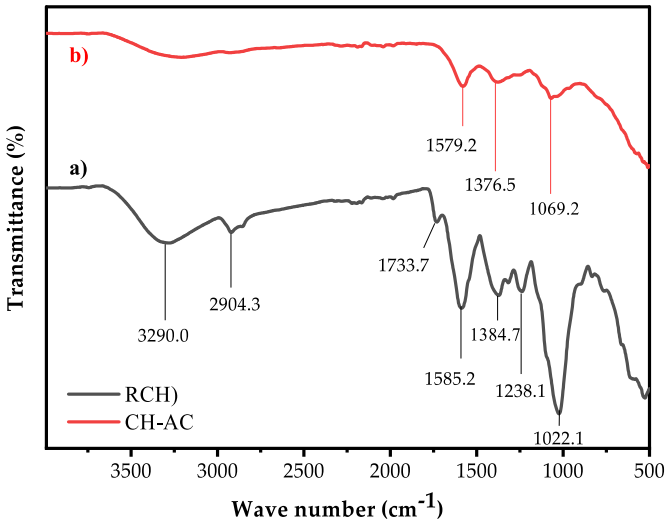

Fig. 2. FTIR spectrum of (a) RCH, and (b) CH-AC treated with $0.8H_3PO_4$ impregnation ratio, 700 °C calcination temperature, and 90 min calcination time.

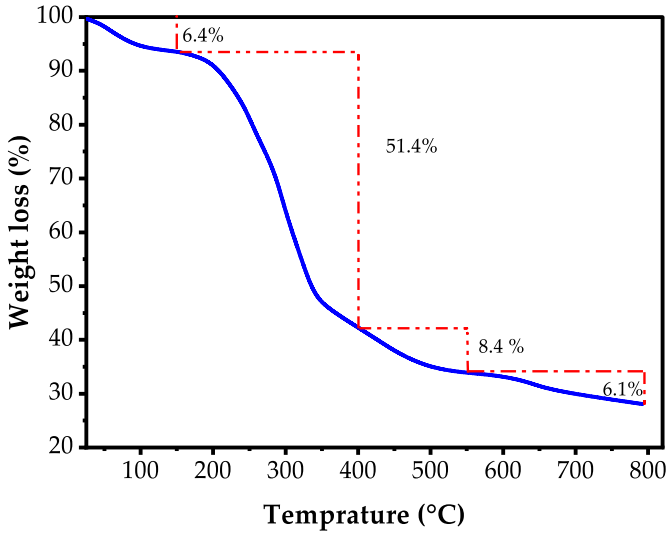

Fig. 3. Thermogravimetric analysis (TGA) for raw castor seed hull.

3.3. Thermogravimetric analysis

The thermogravimetric analysis (TGA) experiment was conducted with an initial mass of 12 mg at a ramping rate of 10 K/min from 25 to 800 °C. Fig. 3 illustrates the thermogravimetric analysis of the raw castor seed hull. The moisture and highly volatile compounds are removed up to a temperature of about 150 °C. In this stage, about 6.4% of the initial pressure was lost. Sharp weight losses were observed when the temperature rises from 200 to 400 °C which eliminates volatile matters and tars due to carbonization or active pyrolysis [14]. In the second stage, about 5.4% of the total initial weight was removed. Previous studies demonstrated that the second stage can be divided into hemicelluloses decomposition range (180–270 °C) and celluloses decomposition range (270–400 °C) [14,31]. The third stage (400–550 °C) with a weight loss of 8.4% corresponds to the decomposition of structurally stable components of the biomass [44]. Beyond 550 °C, less weight loss was observed due to the decomposition of lignin of which decomposition may take place at higher temperatures [14,20,31,44]. The total weight loss at 800 °C is about 72.3% which shows calcination without H_3PO_4 impregnation provides a low AC yield. Similar observations were reported for other biomasses such as almond shells [35], waste tea [35], tomato stem [35], tomato leaves [35], castor bean residue [32], pinewood [2], and acai seed [37].

3.4. XRD analysis

Fig. 4 shows the XRD spectrum of the raw caster seed husk (RCH) and its activated carbon which was activated at 700 CH-AC which was 700 °C. The samples were scanned over 2θ of 10–80° using Cu-Kα

radiation with a wavelength of 1.541874 Å. Both the RCH shows broad reflections in the range of 2θ of 10°–30° that is centered at 24.74°, respectively. It has sharp peaks at 2θ of 43.89°, 64.38°, and 77.44°. This shows the RCH has mainly amorphous characteristics with minor crystal characteristics which might be attributed to its high ash contents. The activated carbon exhibits a broad peak in the range of 2θ from 10° to 30° with the absence of sharp peaks which is a characteristic of well-defined porous materials.

3.5. Activated carbon yields

The activated carbon yield is defined as grams of activated carbon per gram char utilized for activation. The activated carbon yield was calculated using Eq. (2).

$$Yield\ ((\%) = \frac{w_a}{w_p} x100 \tag{2}$$

where, w_a is the weight of the dried activated carbon and w_p is the weight of the dried precursor. As seen in Fig. 5, the AC yield varies from 39.56% to 78.86%. The maximum AC yield of the current precursor is higher than the activated carbon yield reported for other biomass, such as durian shell (45.5 wt%) [34], palm shell (43.5 wt%) [33] coconut shell (50.84.%) [45], and nutshell (68.2%) [46]. However, the maximum yield obtained from the castor seed hull is slightly lower than reported for mangosteen peel which is more than 95% [47]. This shows caster seed husk is one of the potential precursors for the production of activated carbon.

The effect of activation temperature, activation time, and impregnation on the yield of AC is depicted in Fig. 5(a). As it can be seen, the yield of AC sightly decreases with temperature. H_3PO_4 impregnated calcination of biomass pressures provides higher AC at a lower temperature compared to other impregnation agents [33]. Although many of the previous works tried calcination of H_3PO_4 impregnated biomass at higher up to 800 °C, the optimum temperatures are identified in lower temperature ranges [33,45]. For some precursors activated with H_3PO_4 an optimum temperature of around 500 °C was observed. For instance, Heidari et al. [3] observed an optimum calcination temperature of 450 °C for activation of eucalyptus wood, and Xu et al. [48] determined an optimum temperature of 500 °C for reedy grass activation using H3PO4 impregnation.

The effect of H_3PO_4 impregnation ratio (X_p) on the AC yield can be observed in Fig. 5(a). The impregnation ratio was fixed at the lowest possible values (0.25–0.8) minimize to H_3PO_4 consumption for process

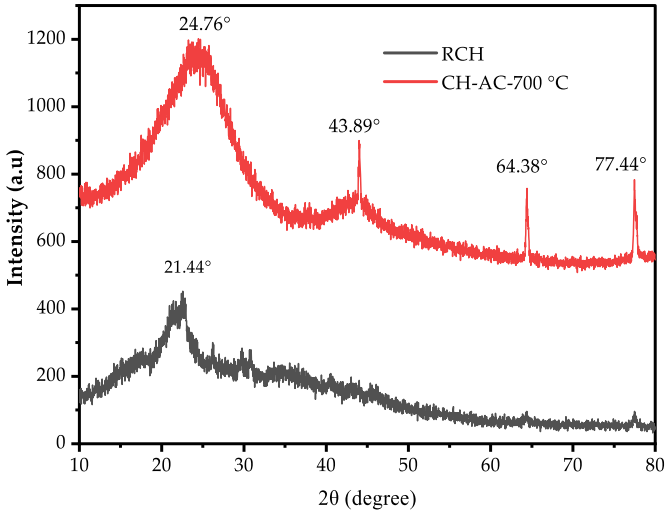

Fig. 4. X-ray diffraction of castor seed hull (a) and its activated carbon (b) AC-700 °C.

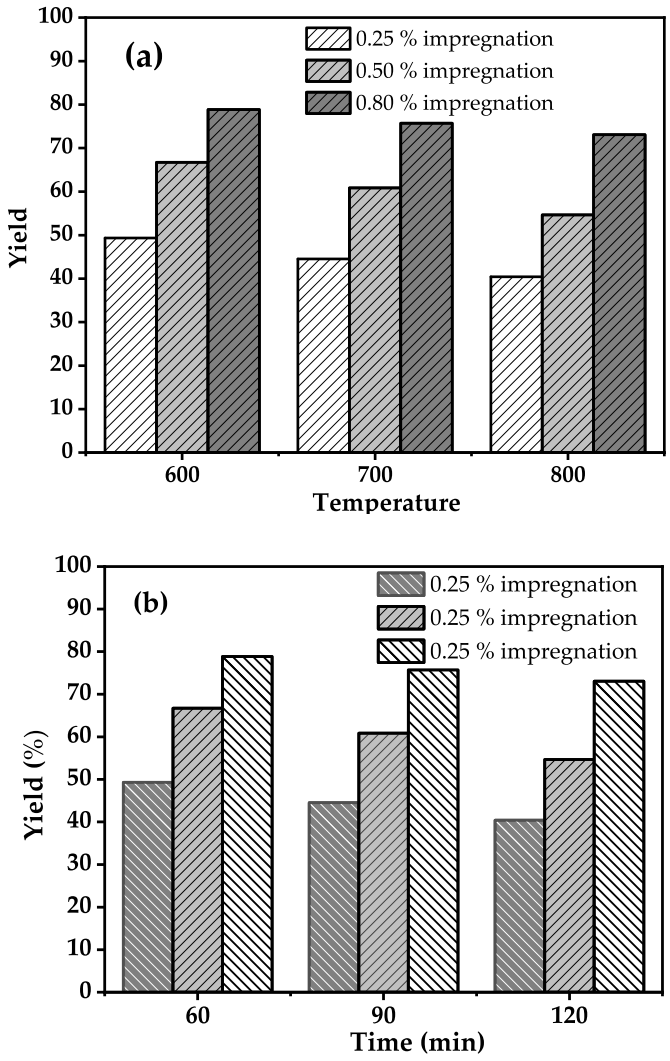

Fig. 5. Effect of Temperature, impregnation ratio, and time on AC yield. (a) Effect of temperature and impregnation ratio; (b) effect of activation time and impregnation ratio.

economic benefits. Impregnation ratio used in this work is much lower than the values reported for different biomasses, such as mangosteen peel (0.25–1.25) [49], palm shell (0.5–3.0) [33], paulownia wood (0.0–4.0) [17] and mangrove (3.0–5.0) [24]. AC yield increases with impregnation ratio as previously reported for many biomass chemical activations [24,33,49]. As the impregnation ratio increases, more H_3PO_4 penetrated deeply into the biomass structure and forms AC [24]. Moreover, it should be noted, that an extreme increase in impregnation ratio may result in a reduction of AC yield as previously observed by González-García [24]. At extremely high H_3PO_4 content, gasification of surface carbon atoms became predominant which may lead to high weight loss and contributed to a low yield of activated carbon [24,50]. Phosphoric acid combines with organic species to form phosphoric linkages, such as phosphate and polyphosphate esters, that result in broader porous structures in AC [51].

Fig. 5 (b) shows the effects of activation time and impregnation ratio on the yield of AC. As it can be seen, the AC yield decreases as the temperature reduced from 60 °C to 120 °C. In general, the optimum activation time for various chemical-based biomass activation ranges from 30 to 120 min depending upon the activation method and the activating agent [33]. Mostly, activation biomass precursors with H_3PO_4 requires less time. For example, H_3PO_4 impregnated optimum activation temperature reported for coconut shell) [45] and rubberwood sawdust

[52] are 60 min and 30 min, respectively. Further increases in activation time beyond the optimum values result in a reduction of AC yield which is in agreement with the current observation [45].

3.6. Textural characteristics of AC

The textural properties of the castor bean husk AC (CH-AC) were characterized by measuring the nitrogen adsorption/desorption isotherms at 77 K. Fig. 6 shows the nitrogen adsorption-desorption capacity with respect to the nitrogen relative pressure (P/P_0) of activated carbon treated at 700 °C for 90 min. A sharp increase in pore volumes at low pressure was observed for the activated carbons which indicates the presence of a higher amount of micropores available with the activated carbons [33]. As the H_3PO_4 impregnation ratio increases from 0.25 to 0.80, the nitrogen adsorption increases, and maximum adoption was obtained for 0.8 acid impregnation. For AC with $0.8H_3PO_4$ impregnation ratio, the pore volume continued to increase as p/p_o increased which indicates the availability of mesopores and the multilayer filling process of N_2 [33]. The adsorption isotherm shape may provide preliminary information on the adsorption mechanism and the porous structure of AC [34]. According to IUPAC isotherms classification [53], the current isotherms may fall into type IV isotherms which show the AC presence of micropores and mesopores. The presence of some mesopores leads to a gradual increase in adsorption after the total filling of the micropores [34]. The pore size distribution is depicted in Fig. 7. For activated carbon impregnated with $0.8H_3PO_4$ a significant portion of the activated pore is in the mesoporous range while for other activated carbon the micropores and mesopores seem balanced.

The presence of both micropore and mesopore structures in the AC can also be observed in Table 5. The mesoporous nature of the active carbon increases with the impregnation ratio which continuously increases nitrogen adsorption after the micropore structure is completely occupied. Moreover, the total pore volume (V_T) of the AC increases with the impregnation ratio, and a maximum V_T of 0.5562 (cm^3/g) was observed at the impregnation ratio (0.80), activation temperature (600 °C), and activation time (60 min). Total pore volume is the volume of liquid nitrogen corresponding to the amount adsorbed at a relative pressure (P/P_o) of 0.99 [17]. The pore volume of the current precursor is comparable with the value reported for other biomasses such as waste bamboo culm (0.451 cm^3/g) [54]. Further, the BET surface area of the AC increases with the impregnation ratio, and a maximum area of 785.38 m^2/g was obtained at the impregnation ratio, activation temperature, and activation time of 0.80, 600 °C, and 60 min, respectively.

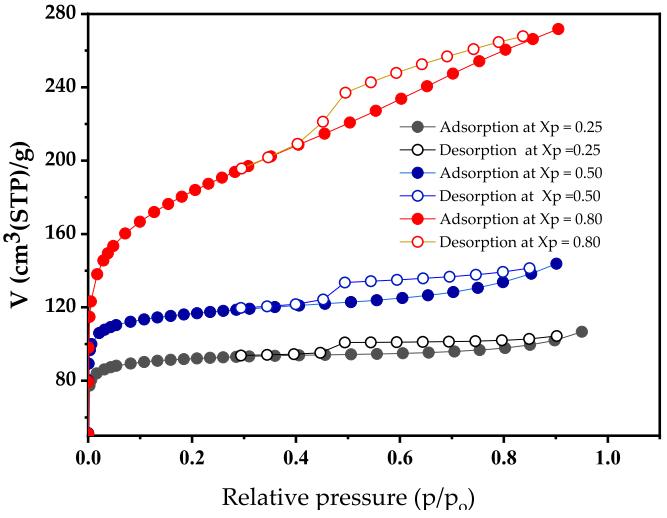

Fig. 6. Adsorption-desorption isotherms of N_2 at 77 K castor seed hull AC at 700 °C for 90 min.

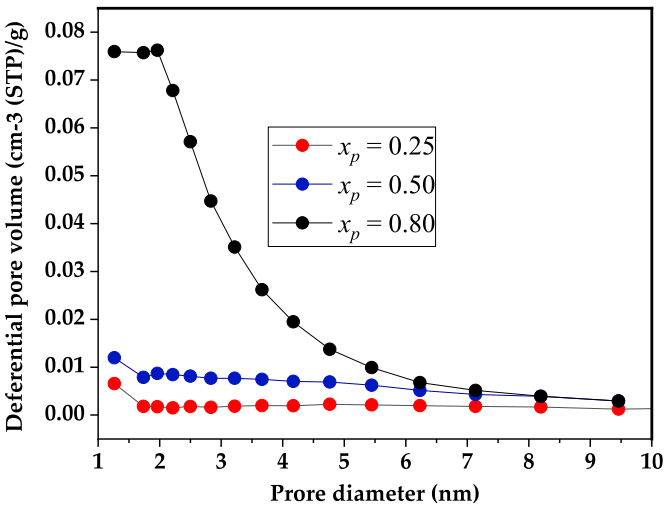

Fig. 7. Pores size distribution of castor seed hull AC activated at 700 °C for 90 min.

Table 5
Textural parameters at a temperature of 600 °C and activation time of 60 min of castor seed activated carbon at different impregnation.

T °C	Time (min)	X_p	Textural parameters				
			S_{BET} (m^2/g)	a_p (m^2/g)	V_{mes} (cm^3/g)	V_T (cm^3/g)	d_p (nm)
600	60	0.525	239.22	37.67	0.0702	0.1571	2.6262
800	60	0.525	318.44	42.04	0.0512	0.1897	2.3826
600	120	0.525	304.74	150.97	0.1993	0.2763	3.6261
800	120	0.525	567.46	194.91	0.2569	0.4310	3.0383
600	90	0.250	298.89	24.892	0.0369	0.1644	2.2003
800	90	0.250	315.64	15.581	0.2925	0.1650	2.0011
600	90	0.800	327.60	126.00	0.1928	0.2946	3.5962
800	90	0.800	589.67	194.32	0.2700	0.4522	3.0678
700	60	0.250	359.20	42.00	0.0505	0.1845	2.0547
700	120	0.500	638.52	199.21	0.2143	0.4203	2.6332
700	60	0.500	400.00	37.67	0.0565	0.2224	2.2239
700	90	0.800	785.38	232.79	0.3052	0.5562	2.8328

S_{BET} =BET surface area, a_p (m^2/g) = surface area, V_{mes} = mesoporous volume/pore volume, V_T = total pore volume, and d_p (nm) = pore diameter.

The BET surface area of the current castor seed hull AC is comparable with the value reported for waste bamboo culm (747 cm^2/g) [54].

4. Conclusion

In this work, the castor bean hull was used as a precursor for AC production through H_3PO_4 impregnation and thermal activation. The effects H_3PO_4, activation temperature, and activation time were studied. The AC yield increases with increasing impregnation ratio while the slightly decreases with activation temperature and activation temperature. Moreover, the BET surface area and pore volume increase with increasing H_3PO_4 impregnation ratio. The impregnation ratio greatly influences the yield AC, its morphology, and textural characteristics. A maximum AC yield of 78.86%, was obtained at $0.8H_3PO_4$ impregnation ratio, activation temperature of 700 °C, and activation time of 60 min. Moreover, a maximum BET surface area of 785.38 m^2/g was obtained at $0.8H_3PO_4$ impregnation ration 78.86%, activation temperature of 700 °C, and activation time of 60 min. The results showed that castor bean hull may be used as a precursor for the synthesis of AC.

Credit author statement

Ibsa Neme: Conceptualization, Methodology/Study design,

Software, ValidationFormal analysis, Investigation, Resources, Data curation, Writing – original draft, Visualization, Funding acquisition; **Girma Gonfa**: Conceptualization, Methodology/Study design, Software, ValidationFormal analysis, Investigation, Resources, Data curation, Writing – review and editing, Visualization, Supervision, Project administration, Funding acquisition; **Chandran Masi:** Conceptualization, Resources, Supervision, Project administration, Funding acquisition.

Declaration of competing interest

The authors declare that they have no known competing financial interests or personal relationships that could have appeared to influence the work reported in this paper.

Acknowledgements

This work is supported by Addis Ababa Science and Technology University.

References

[1] M. Danish, T. Ahmad, A review on utilization of wood biomass as a sustainable precursor for activated carbon production and application, Renew. Sustain. Energy Rev. 87 (2018) 1–21.
[2] M.B. Ahmed, M.A.H. Johir, J.L. Zhou, H.H. Ngo, L.D. Nghiem, C. Richardson, M. A. Moni, M.R. Bryant, Activated carbon preparation from biomass feedstock: clean production and carbon dioxide adsorption, J. Clean. Prod. 225 (2019) 405–413.
[3] A. Heidari, H. Younesi, A. Rashidi, A. Ghoreyshi, Adsorptive removal of CO2 on highly microporous activated carbons prepared from Eucalyptus camaldulensis wood: effect of chemical activation, J. Taiwan Inst. Chem. Eng. 45 (2) (2014) 579–588.
[4] A.E. Ogungbenro, D.V. Quang, K.A. Al-Ali, L.F. Vega, M.R. Abu-Zahra, Synthesis and characterization of activated carbon from biomass date seeds for carbon dioxide adsorption, J. Environ. Chem. Eng. 8 (5) (2020), 104257.
[5] M. Ramamoorthy, S. Ragupathy, D. Sakthi, V. Arun, N. Kannadasan, Enhanced sunlight photodegradation activity of methylene blue using Mn doped SnO2 loaded on corn cob activated carbon, Results Mater. 8 (2020), 100144.
[6] R. Zakaria, N.A. Jamalluddin, M.Z. Abu Bakar, Effect of impregnation ratio and activation temperature on the yield and adsorption performance of mangrove based activated carbon for methylene blue removal, Results Mater. 10 (2021), 100183.
[7] H. Mudoga, H. Yucel, N. Kincal, Decolorization of sugar syrups using commercial and sugar beet pulp based activated carbons, Bioresour. Technol. 99 (9) (2008) 3528–3533.
[8] Z. Juan, F. Kaixuan, W. Pingping, Z. Yue, Z. Yongke, Enhancement of the adsorption of bilirubin on activated carbon via modification, Results Mater. 9 (2021), 100172.
[9] S. Karthikeyan, W.-K. Jo, R. Dhanalakshmi, M.A. Isaacs, K. Wilson, G. Sekaran, A. F. Lee, A porous activated carbon supported Pt catalyst for the oxidative degradation of poly[(naphthaleneformaldehyde)sulfonate], J. Taiwan Inst. Chem. Eng. 93 (2018) 289–297.
[10] M. Jalalah, S. Rudra, B. Aljafari, M. Irfan, S.S. Almasabi, T. Alsuwian, A.A. Patil, A. K. Nayak, F.A. Harraz, Novel porous heteroatom-doped biomass activated carbon nanoflakes for efficient solid-state symmetric supercapacitor devices, J. Taiwan Inst. Chem. Eng. 132 (2021).
[11] G. Wang, B. Qian, Q. Dong, J. Yang, Z. Zhao, J. Qiu, Highly mesoporous activated carbon electrode for capacitive deionization, Separ. Purif. Technol. 103 (2013) 216–221.
[12] A.M. Abioye, F.N. Ani, Recent development in the production of activated carbon electrodes from agricultural waste biomass for supercapacitors: a review, Renew. Sustain. Energy Rev. 52 (2015) 1282–1293.
[13] H. Teng, T.-S. Yeh, L.-Y. Hsu, Preparation of activated carbon from bituminous coal with phosphoric acid activation, Carbon 36 (9) (1998) 1387–1395.
[14] P. González-García, Activated carbon from lignocellulosics precursors: a review of the synthesis methods, characterization techniques and applications, Renew. Sustain. Energy Rev. 82 (2018) 1393–1414.
[15] O. Ioannidou, A. Zabaniotou, Agricultural residues as precursors for activated carbon production—a review, Renew. Sustain. Energy Rev. 11 (9) (2007) 1966–2005.
[16] A. Zubrik, M. Matik, S. Hredzák, M. Lovás, Z. Danková, M. Kováčová, J. Briančin, Preparation of chemically activated carbon from waste biomass by single-stage and two-stage pyrolysis, J. Clean. Prod. 143 (2017) 643–653.
[17] S. Yorgun, D. Yıldız, Preparation and characterization of activated carbons from Paulownia wood by chemical activation with H3PO4, J. Taiwan Inst. Chem. Eng. 53 (2015) 122–131.
[18] Y.J.T.P.A.L.M.A.A.S.-D. Y.H.Taufiq-Yapb, Performances of toluene removal by activated carbon derived from durian shell, Bioresour. Technol. 102 (2) (2011) 724–728.
[19] D. Xin-Hui, C. Srinivasakannan, P. Jin-Hui, Z. Li-Bo, Z. Zheng-Yong, Preparation of activated carbon from Jatropha hull with microwave heating: optimization using response surface methodology, Fuel Process. Technol. 92 (3) (2011) 394–400.
[20] W. Tongpoothorn, M. Sriuttha, P. Homchan, S. Chanthai, C. Ruangviriyachai, Preparation of activated carbon derived from Jatropha curcas fruit shell by simple thermo-chemical activation and characterization of their physico-chemical properties, Chem. Eng. Res. Des. 89 (3) (2011) 335–340.
[21] M. Fan, W. Marshall, D. Daugaard, R. Brown, Steam activation of chars produced from oat hulls and corn stover, Bioresour. Technol. 93 (1) (2004) 103–107.
[22] B.S. Girgis, S.S. Yunis, A.M. Soliman, Characteristics of activated carbon from peanut hulls in relation to conditions of preparation, Mater. Lett. 57 (1) (2002) 164–172.
[23] T. Zhang, W.P. Walawender, L. Fan, M. Fan, D. Daugaard, R. Brown, Preparation of activated carbon from forest and agricultural residues through CO2 activation, Chem. Eng. J. 105 (1–2) (2004) 53–59.
[24] R. Zakaria, N.A. Jamalluddin, M.Z.A. Bakar, Effect of impregnation ratio and activation temperature on the yield and adsorption performance of mangrove based activated carbon for methylene blue removal, Results Mater. 10 (2021), 100183.
[25] N. Oladoja, C. Aboluwoye, Y. Oladimeji, A. Ashogbon, I. Otemuyiwa, Studies on castor seed shell as a sorbent in basic dye contaminated wastewater remediation, Desalination 227 (1–3) (2008) 190–203.
[26] K. Anjani, Castor genetic resources: a primary gene pool for exploitation, Ind. Crop. Prod. 35 (1) (2012) 1–14.
[27] L.S. Severino, D.L. Auld, M. Baldanzi, M.J. Cândido, G. Chen, W. Crosby, D. Tan, X. He, P. Lakshmamma, C. Lavanya, A review on the challenges for increased production of castor, Agron. J. 104 (4) (2012) 853–880.
[28] L.M. Ferreira, R.R. de Melo, A.S. Pimenta, T.K.B. de Azevedo, C.B. de Souza, Adsorption performance of activated charcoal from castor seed cake prepared by chemical activation with phosphoric acid, Biomass Convers. Biorefinery (2020) 1–12.
[29] I. Aldobouni, A. Fadhil, I. Saied, Conversion of de-oiled castor seed cake into bio-oil and carbon adsorbents, Energy Sources, Part A Recovery, Util. Environ. Eff. 37 (24) (2015) 2617–2624.
[30] V. Ospina, R. Buitrago-Sierra, D. López, HDO of guaiacol over NiMo catalyst supported on activated carbon derived from castor de-oiled cake, Ing. Invest. 35 (2) (2015) 49–55.
[31] M. Sánchez-Cantú, V.J. Janeiro-Coronel, J.A. Galicia-Aguilar, J.D. Santamaría-Juárez, Effect of the activation temperature over activated carbon production from castor cake and its evaluation as dye adsorbent, Int. J. Environ. Sci. Technol. 15 (7) (2018) 1521–1530.
[32] L.L. Zhi, M.A.A. Zaini, Adsorption properties of cationic rhodamine B dye onto metals chloride-activated castor bean residue carbons, Water Sci. Technol. 75 (4) (2017) 864–880.
[33] W.C. Lim, C. Srinivasakannan, N. Balasubramanian, Activation of palm shells by phosphoric acid impregnation for high yielding activated carbon, J. Anal. Appl. Pyrol. 88 (2) (2010) 181–186.
[34] T.C. Chandra, M.M. Mirna, J. Sunarso, Y. Sudaryanto, S. Ismadji, Activated carbon from durian shell: preparation and characterization, J. Taiwan Inst. Chem. Eng. 40 (4) (2009) 457–462.
[35] B. Tiryaki, E. Yagmur, A. Banford, Z. Aktas, Comparison of activated carbon produced from natural biomass and equivalent chemical compositions, J. Anal. Appl. Pyrol. 105 (2014) 276–283.
[36] A. Kumar, H.M. Jena, Preparation and characterization of high surface area activated carbon from Fox nut (Euryale ferox) shell by chemical activation with H3PO4, Results Phys. 6 (2016) 651–658.
[37] L.S. Queiroz, L.K.C. de Souza, K.T.C. Thomaz, E.T. Leite Lima, G.N. da Rocha Filho, L.A.S. do Nascimento, L.H. de Oliveira Pires, K.d.C.F. Faial, C.E.F. da Costa, Activated carbon obtained from amazonian biomass tailings (acai seed): modification, characterization, and use for removal of metal ions from water, J. Environ. Manag. 270 (2020), 110868.
[38] M. Kılıç, E. Apaydın-Varol, A.E. Pütün, Preparation and surface characterization of activated carbons from Euphorbia rigida by chemical activation with ZnCl2, K2CO3, NaOH and H3PO4, Appl. Surf. Sci. 261 (2012) 247–254.
[39] A.H. Jawad, A. Saud Abdulhameed, L.D. Wilson, S.S.A. Syed-Hassan, Z. A. Alothman, M. Rizwan Khan, High surface area and mesoporous activated carbon from KOH-activated dragon fruit peels for methylene blue dye adsorption: optimization and mechanism study, Chin. J. Chem. Eng. 32 (2021) 281–290.
[40] A.H. Jawad, M. Bardhan, M.A. Islam, M.A. Islam, S.S.A. Syed-Hassan, S. Surip, Z. A. ALOthman, M.R. Khan, Insights into the modeling, characterization and adsorption performance of mesoporous activated carbon from corn cob residue via microwave-assisted H3PO4 activation, Surface. Interfac. 21 (2020), 100688.
[41] A.H. Jawad, A.M. Kadhum, Y. Ngoh, Applicability of dragon fruit (Hylocereus polyrhizus) peels as low-cost biosorbent for adsorption of methylene blue from aqueous solution: kinetics, equilibrium and thermodynamics studies, Desalination Water Treat. 109 (2018) 231–240.
[42] A.H. Jawad, N.N. Mohd Firdaus Hum, A.S. Abdulhameed, M.A. Mohd Ishak, Mesoporous activated carbon from grass waste via H3PO4-activation for methylene blue dye removal: modelling, optimisation, and mechanism study, Int. J. Environ. Anal. Chem. (2020) 1–17.
[43] A.M. Awad, M.F. Shaffei, O.S. Shehata, H.S. Mandour, H.S. Hussein, Surface. Interfac. (2016).
[44] D. Lozano-Castello, M. Lillo-Ródenas, D. Cazorla-Amorós, A. Linares-Solano, Preparation of activated carbons from Spanish anthracite: I. Activation by KOH, Carbon 39 (5) (2001) 741–749.

[45] Q. Liang, Y. Liu, M. Chen, L. Ma, B. Yang, L. Li, Q. Liu, Optimized preparation of activated carbon from coconut shell and municipal sludge, Mater. Chem. Phys. 241 (2020), 122327.
[46] A.S. Olawale, O.A. Ajayi, M.S. Olakunle, M.T. Ityokumbul, S.S. Adefila, in: Preparation of phosphoric acid activated carbons from Canarium Schweinfurthii Nutshell and its role in methylene blue adsorption, Preparation of phosphoric acid activated carbons from Canarium Schweinfurthii Nutshell and its role in methylene blue adsorption, 6, 2015, pp. 1–6.
[47] K. Foo, B. Hameed, Preparation and characterization of activated carbon from pistachio nut shells via microwave-induced chemical activation, Biomass Bioenergy 35 (7) (2011) 3257–3261.
[48] J. Xu, L. Chen, H. Qu, Y. Jiao, J. Xie, G. Xing, Preparation and characterization of activated carbon from reedy grass leaves by chemical activation with H3PO4, Appl. Surf. Sci. 320 (2014) 674–680.
[49] K. Foo, B. Hameed, Factors affecting the carbon yield and adsorption capability of the mangosteen peel activated carbon prepared by microwave assisted K2CO3 activation, Chem. Eng. J. 180 (2012) 66–74.
[50] P. Patnukao, P. Pavasant, Activated carbon from Eucalyptus camaldulensis Dehn bark using phosphoric acid activation, Bioresour. Technol. 99 (17) (2008) 8540–8543.
[51] Y. Li, X. Zhang, R. Yang, G. Li, C. Hu, The role of H 3 PO 4 in the preparation of activated carbon from NaOH-treated rice husk residue, RSC Adv. 5 (41) (2015) 32626–32636.
[52] C. Srinivasakannan, M. Zailani Abu Bakar, Production of activated carbon from rubber wood sawdust, Biomass Bioenergy 27 (1) (2004) 89–96.
[53] K.S. Sing, Reporting physisorption data for gas/solid systems with special reference to the determination of surface area and porosity (Recommendations 1984), Pure Appl. Chem. 57 (4) (1985) 603–619.
[54] L. Wang, Application of activated carbon derived from 'waste'bamboo culms for the adsorption of azo disperse dye: kinetic, equilibrium and thermodynamic studies, J. Environ. Manag. 102 (2012) 79–87.